Int. J. Solids Structures, 1974, 10, pp. 123–133. Pergamon Press. Printed in Gt. Britain.

DIFFRACTION OF *SH*-WAVES BY AN ELLIPTIC ELASTIC CYLINDER

S. K. DATTA

Department of Mechanical Engineering, University of Colorado, Boulder, Colorado 80302

(*Received* 23 *April* 1973; *revised* 29 *June* 1973)

Abstract—Diffraction of *SH*-waves by an elliptic elastic cylinder has been discussed. Results are derived also for the case of an elliptical cavity. Numerical results are presented for the shear stress on the cylinder.

1. INTRODUCTION

Wave propagation in an elastic medium in the presence of variously shaped inclusions or cavities is of interest in many areas of engineering and geophysics. For reasons of various applications, the diffraction of elastic waves by an inclusion or a cavity has been the subject of several studies in recent years (for a detailed review, see [1]). However, most of these studies are concerned with diffraction by spheres, penny-shaped cracks or discs, circular cylinders and Griffith cracks or rigid ribbons. The reason being that in the mathematical analysis of diffraction problems, conventional techniques are limited to examples exhibiting strong geometric symmetry.

In an earlier paper[2] we have used the method of matched asymptotic expansions to solve the problem of diffraction of a *P*-wave by a rigid spheroidal inclusion. We presented both the near- and far-field solutions and then presented numerical results for the far-field displacement, stress distribution on the inclusion and the response of the inclusion. Various limiting solutions that can be obtained from the spheroidal solution are discussed in [3] and have been shown to agree with the exact solutions. It was found in [2, 3] that the expansion of the displacement field for small wave numbers ε is a power series in ε.

In the present paper we have used the same technique to solve the diffraction of *SH*-waves by an elliptic elastic cylindrical inclusion. In this case, not only terms of $0(\varepsilon^p)$ appear but also those of $0(\varepsilon^p(\ln \varepsilon)^q)$. So the analysis is not as direct as in the three dimensional case and thus is of some interest. Besides, the problem does not have a suitable exact solution (see [1], pp. 446–451). In the case when elliptic inclusion is a cavity or when it is rigid, formal solutions can be found (see [1], pp. 440–446). However, no numerical results have been reported. Harper[4] has presented the solution for acoustic diffraction by a cylindrical cavity by using the technique of matched asymptotic expansion. In that case the expansion comes out to be in powers of $1/\ln \varepsilon$ and is different from ours.

2. EQUATIONS

Consider an elastic elliptic cylinder of rigidity μ_1' embedded in an infinite elastic medium of rigidity μ_1. We shall assume that the inclusion is in welded contact with the surrounding medium. Let the z-axis be along the axis of the cylinder. Define elliptical coordinates in a plane perpendicular to the z-axis as

$$x = c\cosh\xi\cos\eta, \qquad y = c\sinh\xi\sin\eta$$
$$\xi_0 \le \xi < \infty, \qquad -\pi \le \eta \le \pi. \tag{1}$$

The boundary of the ellipse is given by $\xi = \xi_0$.

Suppose that a plane SH-wave is incident along the y-axis. The displacement field associated with the incident wave is given by

$$u_x^{(i)} = u_y^{(i)} = 0, \qquad u_z^{(i)} = W^{(i)} = W_0 \mathrm{e}^{ik(y - C_2 t)}. \tag{2}$$

Here $k = \omega/C_2$, C_2 being the shear wave speed in the matrix and $\omega/2\pi$ is the frequency. The complete wave outside the cylinder will be denoted by

$$\mathrm{e}^{-i\omega t}W = W^{(i)}/W_0 + W^{(\mathrm{sc})}/W_0 \tag{3}$$

and that inside the cylinder by

$$\mathrm{e}^{-i\omega t}W' = W^{(\mathrm{tr})}/W_0. \tag{4}$$

Then W and W' satisfy the equations

$$\frac{1}{h^2}\left(\frac{\partial^2}{\partial\xi^2} + \frac{\partial^2}{\partial\eta^2}\right)W + k^2 W = 0 \tag{5}$$

$$\frac{1}{h^2}\left(\frac{\partial^2}{\partial\xi^2} + \frac{\partial^2}{\partial\eta^2}\right)W' + k'^2 W = 0 \tag{6}$$

$$h^2 = c^2(\cosh^2\xi - \cos^2\eta)$$

with $k' = \omega/C_2'$, C_2' being the shear wave speed inside the cylinder. The boundary conditions on $\xi = \xi_0$ are

$$W = W', \qquad \xi = \xi_0$$
$$\mu_1 \frac{\partial W}{\partial\xi} = \mu_1' \frac{\partial W'}{\partial\xi}, \qquad \xi = \xi_0. \tag{7}$$

Besides $W^{(\mathrm{sc})}$ must satisfy the radiation condition at infinity.

3. SOLUTION

We shall solve (5) and (6) for small values of $\varepsilon(= kc)$ and $\varepsilon'(= k'c)$. For this purpose, we introduce the inner expansions as

$$W = 1 + \nu_1(\varepsilon)W_1 + \nu_2(\varepsilon)W_2 + \ldots$$
$$W' = 1 + \nu_1(\varepsilon)W_1' + \nu_2(\varepsilon)W_2' + \ldots. \tag{8}$$

For the outer expansion, we assume

$$W = \mathrm{e}^{i\tilde{y}} + \Delta_1(\varepsilon)w_1(\tilde{p}, \eta) + \Delta_2(\varepsilon)w_2 + \ldots \tag{9}$$

where

$$\tilde{y} = \varepsilon y/c = \varepsilon\bar{y}, \qquad \tilde{p} = \varepsilon\sinh\xi. \tag{10}$$

In terms of outer variables W satisfies the equation

$$\mathscr{L}w \equiv \left(\frac{\partial^2}{\partial\tilde{p}^2} + \frac{1}{\tilde{p}}\frac{\partial}{\partial\tilde{p}} + \frac{1}{\tilde{p}^2}\frac{\partial^2}{\partial\eta^2} + 1\right)w = -\frac{\varepsilon^2}{\tilde{p}^2}\left(\sin^2\eta + \frac{\partial^2}{\partial\tilde{p}^2}\right)w. \tag{11}$$

For matching we shall introduce the intermediate variables

$$y_\delta = \tilde{y}\delta(\varepsilon) = \tilde{y}\frac{\delta}{\varepsilon}, \qquad p_\delta = \tilde{p}\frac{\delta}{\varepsilon}, \qquad \varepsilon \ll \delta \ll 1. \tag{12}$$

It is easily shown that

$$\begin{aligned} v_1(\varepsilon) &= \varepsilon \\ W_1 &= i\tilde{y} + D_{11}e^{-\xi}\sin\eta \\ W_1' &= D_{11}'\sinh\xi\sin\eta \end{aligned} \tag{13}$$

with

$$D_{11} = -i\frac{(1-\bar{\mu})e^{\xi_0}\sinh\xi_0\cosh\xi_0}{\Delta(\xi_0)}$$

$$D_{11}' = i\frac{\bar{\mu}e^{\xi_0}}{\Delta(\xi_0)}, \qquad \Delta(\xi_0) = \cosh\xi_0 + \sinh\xi_0\,\bar{\mu}, \qquad \bar{\mu} = \mu_1/\mu_1'.$$

Writing equation $(13)_1$ in terms of intermediate variables and expanding in powers of δ, we get

$$W_1 = ip_\delta\sin\eta/\delta + \tfrac{1}{2}D_{11}\frac{\delta}{p_\delta}\sin\eta + 0(\delta^3). \tag{14}$$

To find w_1 let us take $\Delta_1(\varepsilon) = \varepsilon^2$. Then we see from equation (11) that

$$\mathscr{L}w_1 = 0, \tag{15}$$

the solution of which we take as

$$w_1 = a_{10}H_0^{(1)}(\tilde{p}) + a_{11}H_1^{(1)}(\tilde{p})\sin\eta. \tag{16}$$

Writing in terms of intermediate variables and expanding in powers of ε/δ, equation (16) gives

$$\begin{aligned} w_1 = -\frac{2i}{\pi}\Bigg[&\frac{\delta a_{11}}{\varepsilon p_\delta}\sin\eta - \frac{\varepsilon p_\delta}{2\delta}\ln\left(\frac{\varepsilon p_\delta}{\delta}\right)a_{11}\sin\eta - a_{10}\ln\left(\frac{\varepsilon p_\delta}{\delta}\right) - \left(\gamma - \ln 2 - \frac{i\pi}{2}\right)a_{10} \\ &+ a_{11}\frac{\varepsilon p_\delta}{\delta}\left(\frac{i\pi}{4} + \frac{1}{4} - \frac{\gamma}{2} + \frac{1}{2}\ln 2\right)\sin\eta + \frac{1}{4}\frac{\varepsilon^2 p_\delta^2}{\delta^2}\ln\left(\frac{\varepsilon p_\delta}{\delta}\right)a_{10} + 0(\varepsilon^2/\delta^2)\Bigg]. \end{aligned} \tag{17}$$

Here γ is the Euler's constant, 0·5772. For matching to $0(\varepsilon\delta)$, we see that $a_{11} = (i\pi/4)D_{11}$.

Next we choose $v_2(\varepsilon) = \varepsilon^2\ln\varepsilon$, $v_3(\varepsilon) = \varepsilon^2$ with

$$W_2 = D_{20} = W_2', \tag{18}$$

and

$$W_3 = -\tfrac{1}{2}\bar{y}^2 + D_{30} + C_{30} + D_{32}\,e^{-2\xi}\cos 2\eta$$
$$W_3' = -\frac{1}{8}\frac{\mu_1\rho_1'}{\mu_1'\rho_1}(\cosh 2\xi + \cos 2\eta) + C_{30}' + D_{32}'\cosh 2\xi\cos 2\eta. \tag{19}$$

From equation $(19)_1$ we get

$$W_3 = -\tfrac{1}{2}y_\delta^2/\delta^2 + D_{30}\left[\ln\frac{p_\delta}{\delta} + \ln 2 + \tfrac{1}{4}\delta^2/p_\delta^2\right] + C_{30} + \tfrac{1}{4}D_{32}\frac{\delta^2}{p_\delta^2}\cos 2\eta + 0(\delta^4/p_\delta^4). \tag{20}$$

Thus for matching to $0(\varepsilon^2)$ we set

$$a_{10} = -\frac{i\pi}{2}D_{30}$$
$$C_{30} = D_{30}[\gamma - 2\ln 2 - i\pi/2] \tag{21}$$
$$D_{20} = D_{30}.$$

The constants D_{30}, D_{32}, C_{30}', D_{32}' are determined from the boundary conditions on $\xi = \xi_0$ as

$$D_{32} = \frac{e^{2\xi_0}\sinh 2\xi_0[\cosh 2\xi_0(\bar{\mu} - 1) + 1 - \bar{\rho}^{-1}]}{8\Delta'}$$
$$D_{32}' = \frac{\cosh 2\xi_0 + \bar{\mu}\sinh 2\xi_0 - 1 + \bar{\mu}/\bar{\rho}}{8\Delta'} \tag{22}$$

$$\bar{\mu} = \mu_1/\mu_1', \qquad \bar{\rho} = \rho_1/\rho_1', \qquad \Delta' = \sinh 2\xi_0 + \bar{\mu}\cosh 2\xi_0$$

$$D_{30} = \frac{1}{4}\frac{\bar{\rho} - 1}{\bar{\rho}}\sinh 2\xi_0$$
$$C_{30}' = C_{30} + D_{30}\,\xi_0 + \tfrac{1}{8}[\cosh 2\xi_0(\bar{\mu}/\bar{\rho} - 1) + 1]. \tag{23}$$

Note that when $\bar{\rho} = 1$, D_{30}, and hence a_{10}, C_{30} and D_{20} vanish.

Proceeding in this manner, it can be shown that

$$W = 1 + \varepsilon W_1 + \varepsilon^2\ln\varepsilon W_2 + \varepsilon^2 W_3 + \varepsilon^3\ln\varepsilon W_4 + \varepsilon^3 W_5 + \varepsilon^4(\ln\varepsilon)^2 W_6 + \varepsilon^4\ln\varepsilon W_7 + 0(\varepsilon^4). \tag{24}$$

W' has a similar expansion. W_4–W_7 and W_4'–W_7' are given by

$$W_4 = i\frac{a_{11}}{\pi}\sinh\xi\sin\eta + D_{41}e^{-\xi}\sin\eta$$
$$W_4' = D_{41}'\sinh\xi\sin\eta \tag{25}$$

$$W_5 = -\frac{i}{6}\bar{y}^3 + \sinh\xi\sin\eta(C_{51} - \tfrac{1}{4}D_{11})$$
$$+ \sin\eta(D_{51}e^{-\xi} - \tfrac{1}{32}D_{11}e^{-3\xi}) + \sin 3\eta(D_{53}e^{-3\xi} - \tfrac{1}{32}D_{11}e^{-\xi})$$
$$W_5' = \sin\eta\left[D_{51}'\sinh\xi - \frac{\bar{\mu}}{32\bar{\rho}}D_{11}'\sinh 3\eta\right] \tag{26}$$
$$+ \sin 3\eta\left[D_{53}'\sinh 3\xi - \frac{\bar{\mu}}{32\bar{\rho}}D_{11}'\sinh\xi\right]$$

$$W_6 = W_6' = D_{70} \tag{27}$$

$$\begin{aligned} W_7 &= -\frac{i}{4\pi} a_{10}(\cosh 2\xi + \cos 2\eta) + D_{70}\xi + C_{70} + D_{72}e^{-2\xi}\cos 2\eta \\ W_7' &= -\frac{i}{4\pi}\frac{\bar{\mu}}{\bar{\rho}} a_{10}(\cosh 2\xi + \cos 2\eta) + C_{70}' + D_{72}'\cosh 2\xi \cos 2\eta. \end{aligned} \tag{28}$$

The outer expansion is obtained as

$$\begin{aligned} w = e^{i\tilde{y}} &+ \varepsilon^2[a_{10}H_0^{(1)}(\tilde{p}) + a_{11}H_1^{(1)}(\tilde{p})\sin\eta] \\ &+ \varepsilon^4 \ln \varepsilon[a_{20}H_0^{(1)}(\tilde{p}) + a_{21}H_1^{(1)}(\tilde{p})\sin\eta] + 0(\varepsilon^4), \end{aligned} \tag{29}$$

a_{20} and a_{21} are given in the appendix.

As a limiting case of the above analysis, one can now derive the solution for the circular cylindrical inclusion. This limit is obtained by letting $c \to 0$ and ξ, $\xi_0 \to \infty$ such that $ce^{\xi} \to 2r$, $ce^{\xi_0} \to 2a$, where r is the distance from the center and a is the radius of the cylinder. Writing $\varepsilon = ka$, we obtain

$$\begin{aligned} w = e^{i\tilde{y}} &+ \varepsilon^2[a_{10}H_0^{(1)}(\tilde{r}) + a_{11}H_1^{(1)}(\tilde{r})\sin\theta] \\ &+ \varepsilon^4 \ln \varepsilon[a_{20}H_0^{(1)}(\tilde{r}) + a_{21}H_1^{(1)}(\tilde{r})\sin\theta] + 0(\varepsilon^4). \end{aligned} \tag{30}$$

W is given by the same expansion (equation 24) with the new definition of ε and W_1–W_7 are given in the appendix. It is easily shown that these expansions agree with the expansions of the exact solution

$$W = e^{i\tilde{y}} + \sum_{n=0}^{\infty} A_{2n}H_{2n}^{(1)}(\tilde{r})\cos 2n\theta + \sum_{n=0}^{\infty} A_{2n+1}H_{2n+1}^{(1)}(\tilde{r})\sin(2n+1)\theta \tag{31}$$

in terms of the near-field and far-field variables. Here

$$A_{2n} = \varepsilon_{2n}\frac{\varepsilon' J_{2n}'(\varepsilon')J_{2n}(\varepsilon) - \bar{\mu}\varepsilon J_{2n}'(\varepsilon)J_{2n}(\varepsilon')}{\bar{\mu}\varepsilon H_{2n}^{(1)\prime}(\varepsilon)J_{2n}(\varepsilon') - \varepsilon' J_{2n}'(\varepsilon')H_{2n}^{(1)}(\varepsilon)}.$$

A_{2n+1} is obtained from A_{2n} by changing $2n$ to $2n+1$ and multiplying the resulting expression by i.

$$\begin{aligned} \varepsilon_n &= 1, \qquad n = 0 \\ &= 2, \qquad n \neq 0. \end{aligned}$$

We can also derive the expansions for the field scattered by an elliptical cavity by using the appropriate values of the constants. These are also given in the Appendix. As a limiting case of the elliptical cavity, one can now find the solution for the Griffith crack by letting $\xi_0 \to 0$. One obtains

$$\begin{aligned} &D_{11} = i, \qquad a_{11} = -\pi/4, \qquad a_{10} = 0 \\ &W_2 = W_3 = 0, \qquad D_{41} = -i/4, \qquad D_{51} = C_{51} + 3i/32 \\ &C_{51} = \frac{i}{4}\left[2\ln 2 - \gamma + \frac{1}{2} + \frac{i\pi}{2}\right] \\ &D_{53} = \frac{i}{96}, \qquad W_6 = W_7 = 0, \qquad a_{21} = \pi/16, \qquad a_{20} = 0. \end{aligned} \tag{32}$$

Thus

$$W = 1 + i\varepsilon[\bar{y} + e^{-\xi}\sin\eta] - \frac{i}{4}\varepsilon^3 \ln\varepsilon[\bar{y} + e^{-\xi}\sin\eta]$$
$$+ \varepsilon^3\left[-\frac{i}{6}\bar{y}^3 + \sin\eta\sinh\xi\left(C_{51} - \frac{i}{4}\xi\right)\right. \tag{33}$$
$$\left. + \sin\eta\left(D_{51}e^{-\xi} - \frac{i}{32}e^{-3\xi}\right) + \frac{i}{96}\sin 3\eta(e^{-3\xi} - 3ie^{-\xi})\right] + 0(\varepsilon^5 \ln\varepsilon).$$

This agrees with the result derived in [5].

In the foregoing analysis, we have presented the results of an *SH*-wave incident along the minor axis of the ellipse. However, it is a straightforward matter to extend it to include the general incidence. In fact, when the wave is incident at an angle W, w will be given by the same expansions (equations 24 and 29). Of course, W_i's will be more complicated and the constants will be different.

4. NUMERICAL RESULTS AND DISCUSSION

In Figs. 1–4 we have plotted $|\tau_{\xi z}/\tau_0|$ and $|\tau_{\eta z}/\tau_0|$ on $\xi = \xi_0$ for two types of composites and for the scattering by a cavity. Here $\tau_0 = i\varepsilon\mu_1 W_0/c$. The matrix materials have been taken to be aluminum and polymethyl methacrylate (PMMA) and the inclusions are taken to be made of tungsten and 302 stainless steel, respectively. The values have been plotted against $\varepsilon_1 = \varepsilon \cosh\xi_0$ for different ξ_0. Note that in the limit when $c \to 0$, $\xi_0 \to \infty$ such that $c\cosh\xi_0 = a$, ε_1 becomes ka.

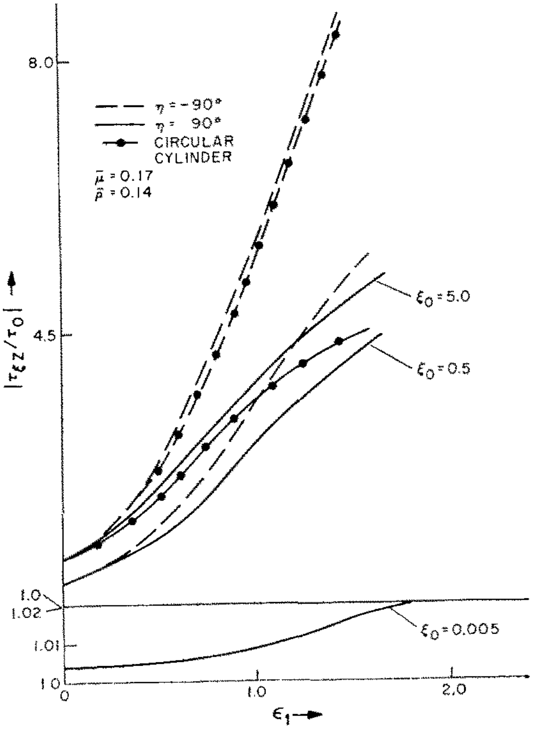

Fig. 1. Plot of $|\tau_{\xi z}/\tau_0|$ against ε_1 for different ξ_0 for Composite I at $\eta = \pm 90°$.

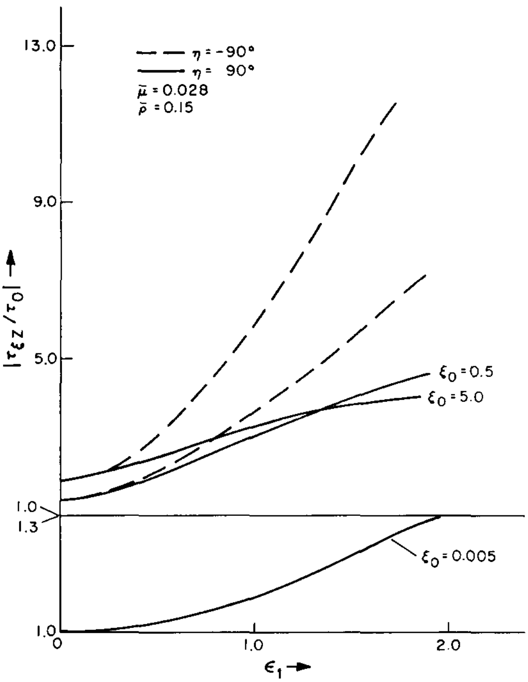

Fig. 2. Plot of $|\tau_{\xi z}/\tau_0|$ against ε_1 for different ξ_0 for Composite II at $\eta = \pm 90°$.

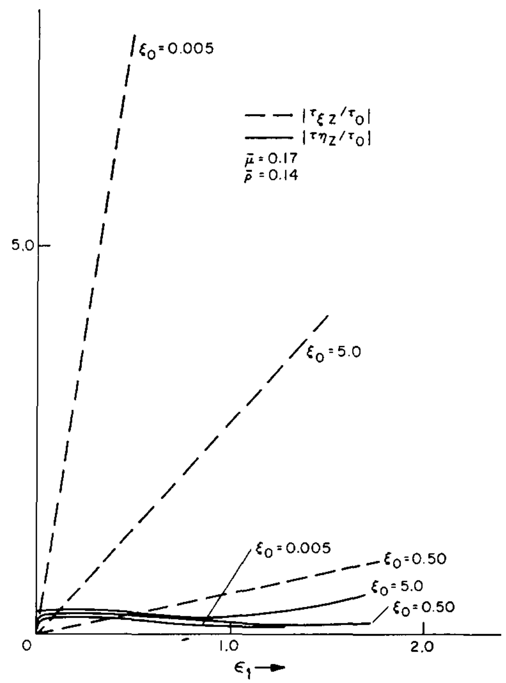

Fig. 3. Plot of $|\tau_{\xi z}/\tau_0|$ against ε_1 for different ξ_0 for Composite I at $\eta = 0°$.

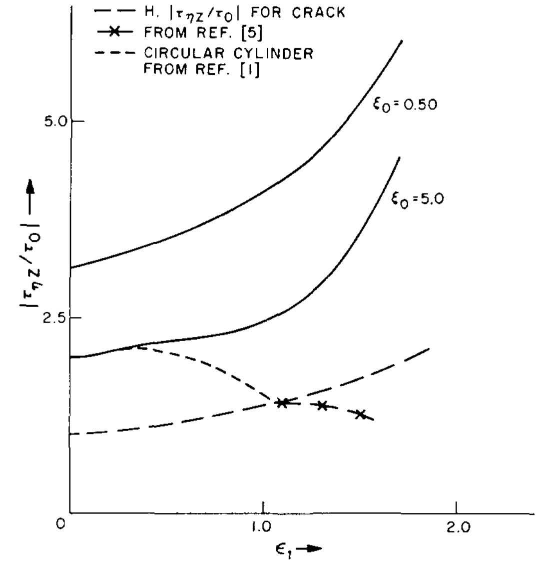

Fig. 4. Plot of $|\tau_{\eta z}/\tau_0|$ against ε_1 at $\eta = 0°$ on an elliptical cavity.

Figure 1 shows the variations of $|\tau_{\xi z}/\tau_0|$ in the matrix for Composite I (tungsten fibre embedded in aluminum matrix). Note that in this case $\bar{\mu} = 0{\cdot}17$ and $\bar{\rho} = 0{\cdot}14$. It is seen that for $\xi_0 \geq 5{\cdot}0$, the results agree very well with those for the circle to the same order of approximation. This is also found to be true for the Composite II (302 stainless steel fibres in PMMA matrix, see Fig. 2). For Composite II $\bar{\mu} = 0{\cdot}028$ and $\bar{\rho} = 0{\cdot}15$. Thus Composite II has almost the same density ratio, but its rigidity ratio is about one-sixth that of I. It is seen that for small ε_1 $|\tau_{\xi z}/\tau_0|$ at $\eta = +90°$ is larger for Composite II than for Composite I. However, this trend is reversed for larger ε_1. For both cases, we find that $|\tau_{\xi z}/\tau_0|$ is larger for positive ε_1 on the illuminated side than on the shadow side. Figures 1 and 2 show that at $\eta = -90°$, this ratio increases much more rapidly than at $\eta = +90°$.

Figure 3 shows the variation of $|\tau_{\xi z}/\tau_0|$ and $|\tau_{\eta z}/\tau_0|$ at $\eta = 0°$ for Composite I. It is seen that $|\tau_{\xi z}/\tau_0|$ increases very rapidly for small ξ_0. It is of interest to point out that $|\tau_{\xi z}/\tau_0|$ first decreases with increasing ξ_0 and then increases. On closer examination of $\tau_{\xi z}/\tau_0$, we find that for small ε and at $\eta = 0°$,

$$\tau_{\xi z}/\tau_0 = -\frac{i\varepsilon}{h}(D_{30} - 2D_{32}\,\mathrm{e}^{-2\xi_0}) + 0(\varepsilon^3 \ln \varepsilon).$$

Thus, for small ξ_0 and small ε

$$\tau_{\xi z}/\tau_0 \simeq +\frac{i\varepsilon}{2\bar{\rho}}(1 - 1/\bar{\mu}) \quad \text{at} \quad \eta = 0°.$$

If we let $\xi_0 \to \infty$ with $c \cosh \xi_0 \to a$, $\varepsilon \to ka$, we get

$$\tau_{\xi z}/\tau_0 \simeq -\frac{i\varepsilon}{2}\left[\frac{2}{1+\bar{\mu}} - \frac{1}{\bar{\rho}}\right] \quad \text{at} \quad \eta = 0°.$$

Thus, for small $\bar{\mu}$ and $\bar{\rho}$, $\tau_{\xi z}/\tau_0$ changes from negative to positive. Furthermore, $|\tau_{\xi z}/\tau_0|_{\xi=\xi_0}$ at $\eta = 0°$ increases with decreasing $\bar{\mu}$ when $\xi_0 \to 0$. On the other hand, it decreases with decreasing $\bar{\mu}$ when ξ_0 is large.

Figure 4 shows the variation of $|\tau_{\eta z}/\tau_0|$ at $\eta = 0°$ for an elliptical cavity. Also shown are the graphs for a circle from [1]. We have also shown the low frequency results for a Griffith crack from [5]. In plotting for the crack, we have multiplied $|\tau_{\eta z}/\tau_0|$ by $h(h = \sinh \xi_0)$. This is done because $|\tau_{\eta z}/\tau_0|$ at $\eta = 0°$ becomes singular like $1/\sinh \xi_0$ when $\xi_0 \to 0$. Note that

$$\lim_{\substack{\eta\to 0\\ \xi_0\to 0}} |\tau_{\eta z}/\tau_0| \neq \lim_{\substack{\xi_0\to 0\\ \eta\to 0}} |\tau_{\eta z}/\tau_0|.$$

We see from Fig. 4 that the low frequency expansion correct to $0(\varepsilon^3 \ln \varepsilon)$ agrees well with the exact solution for the circle up to $\varepsilon_1 = 0{\cdot}4$. The agreement with the expansion to $0(\varepsilon^4 \ln \varepsilon)$ for the crack is good up to $\varepsilon = 1{\cdot}2$. It was shown in [5] that the expansion to $0(\varepsilon^4 \ln \varepsilon)$ agrees well with the exact solution up to $\varepsilon = 0{\cdot}6$. So our result also agrees with the exact solution within this range. To get a better agreement one would have to keep many more terms in the low frequency expansion. This suggests that the low frequency expansion presented in this paper accurately predicts the behavior in $0 \leq \varepsilon \cosh \xi_0 \leq 0{\cdot}4$ for all ξ_0. For $\varepsilon \cosh \xi_0 > 0{\cdot}4$, the expansion agrees better for smaller ξ_0.

5. CONCLUSION

Matched asymptotic expansions have been used to obtain the near and far field distributions of the displacement when *SH*-waves are scattered by one elastic elliptic cylinder. The analysis is valid when the wave number ε is less than one and it has been found that the expansion to $0(\varepsilon^4 \ln \varepsilon)$ gives accurate results for all values of ξ_0 if $\varepsilon \cosh \xi_0 \leq 0{\cdot}4$. The approximation gets better the smaller ξ_0 is. To get an estimate of the frequency range in which this expansion gives good results, we note that for most materials C_2 is $0(10^5$ cm/sec) or larger. So $\varepsilon \cosh \xi_0 = 0{\cdot}4$ corresponds to ω $0(0{\cdot}4 \times 10^5$ cycles/sec) or larger if $C \cosh \xi_0 = 1$ cm.

Although the above analysis considers diffraction of *SH*-waves, the more general problem of diffraction of *P*- and *S*-waves can be solved in a similar manner.

REFERENCES

1. C. C. Mow and Y. H. Pao, *The Diffraction of Elastic Waves and Dynamic Stress Concentrations*, Rand Corporation Report # R-482-PR (1971).
2. S. K. Datta and J. D. Sangster, Response of a rigid spheroidal inclusion to an incident plane compressional elastic wave. *SIAM J. appl. Math.* to be published.
3. ———, *Response of a Rigid Spheroidal Inclusion to an Incident Plane Compressional Elastic Wave*. Report # CUMER-73-1, Feb. (1973), Department of Mechanical Engineering, University of Colorado.
4. E. Y. Harper, Diffraction of plane acoustic waves and pulses as a singular perturbation problem. *J. Math. Phys.* **10**, 1795–1803 (1969).
5. A. K. Mal, A note on the low frequency diffraction of elastic waves by a Griffith crack. *Int. J. Engng. Sci.* **10**, 609–612 (1972).

APPENDIX

$$C_{51} = \tfrac{1}{4}D_{11}[2\ln 2 + \tfrac{1}{2} - \gamma + i\pi/2]$$

$$a_{21} = \frac{i\pi}{4} D_{41}, \qquad a_{20} = -\frac{i\pi}{2} D_{70}$$

$$C_{70} = D_{70}(\gamma - 2\ln 2 - i\pi/2) + ia_{10}/4\pi$$

$$D_{41} = \frac{i}{4}(D_{11})^2, \qquad D_{41}' = \frac{i}{4} D_{11}D_{11}'$$

$$D_{70} = \frac{ia_{10}}{2\pi\bar{\rho}} \sinh 2\xi_0(\bar{\rho} - 1) = (D_{30})^2$$

$$D_{72} = \frac{ia_{10}}{4\pi} e^{2\xi_0}(1 - \bar{\mu}/\bar{\rho})/[1 + \bar{\mu}\coth 2\xi_0]$$

$$D_{72}' = -\frac{ia_{10}}{4\pi} \bar{\mu}(1 - \bar{\mu}/\bar{\rho})/[\sinh 2\xi_0 + \bar{\mu}\cosh 2\xi_0]$$

$$D_{51} = -e^{\xi_0}\Big[\frac{i}{8}(3\bar{\mu} - 1)\sinh^3\xi_0\cosh\xi_0 - \tfrac{1}{32}D_{11}e^{-3\xi_0}(3\bar{\mu}\sinh\xi_0 + \cosh\xi_0)$$
$$- \sinh\xi_0\cosh\xi_0(C_{51} - \tfrac{1}{4}D_{11}\xi_0)(\bar{\mu} - 1) + \tfrac{1}{4}D_{11}\bar{\mu}\sinh^2\xi_0$$
$$- \frac{\bar{\mu}}{32\bar{\rho}} D_{11}'(\sinh\xi_0\cosh 3\xi_0 - 3\cosh\xi_0\sinh 3\xi_0)\Big]\Big/\Delta$$

$$D_{51}' = \bar{\mu}\Big[-\frac{i}{8}\sinh^2\xi_0(\sinh\xi_0 + 3\cosh\xi_0) + \tfrac{1}{16}D_{11}e^{-3\xi_0} + e^{\xi_0}(C_{51} - \tfrac{1}{4}D_{11}\xi_0)$$
$$- \tfrac{1}{4}D_{11}\sinh\xi_0 + \frac{1}{32\bar{\rho}} D_{11}'(3\cosh 3\xi_0 + \bar{\mu}\sinh 3\xi_0)\Big]\Big/\Delta$$

$$D_{53} = -e^{3\xi_0}\Big[\frac{i}{8}\sinh^2\xi_0(\sinh\xi_0\cosh 3\xi_0 - \bar{\mu}\cosh\xi_0\sinh 3\xi_0)$$
$$- \tfrac{1}{32}D_{11}e^{-\xi_0}(3\cosh 3\xi_0 + \bar{\mu}\sinh 3\xi_0)$$
$$+ \frac{\bar{\mu}}{32\bar{\rho}} D_{11}'(3\sinh\xi_0\cosh 3\xi_0 - \cosh\xi_0\sinh 3\xi_0)\Big]\Big/\Delta''$$

$$D_{53}' = \bar{\mu}\Big[\frac{i}{8}\sinh^2\xi_0 e^{\xi_0} - \tfrac{1}{16}D_{11}e^{-\xi_0} + \frac{1}{32\bar{\rho}} D_{11}'(3\bar{\mu}\sinh\xi_0 + \cosh\xi_0)\Big]\Big/\Delta''$$

$$\Delta'' = 3(\cosh 3\xi_0 + \bar{\mu}\sinh 3\xi_0).$$

For the scattering by a circular cylindrical inclusion, we get

$$W_1 = i\bar{y} + \frac{D_{11}}{\bar{r}}\sin\theta, \qquad W_1' = D_{11}'\bar{r}\sin\theta, \qquad \bar{r} = r/a$$

$$D_{11} = i\frac{\bar{\mu} - 1}{\bar{\mu} + 1}, \qquad D_{11}' = i\frac{2\bar{\mu}}{\bar{\mu} + 1}$$

$$W_2 = W_2' = D_{30}$$

$$W_3 = -\tfrac{1}{2}\bar{y}^2 + D_{30}\ln\bar{r} + C_{30} + D_{32}\frac{1}{\bar{r}^2}\cos 2\theta$$

$$C_{30} = D_{30}(\gamma - \ln 2 - i\pi/2)$$

$$D_{30} = \frac{1}{2}\frac{\bar{\rho}-1}{\bar{\rho}}, \qquad D_{32} = \frac{1}{4}\frac{\bar{\mu}-1}{\bar{\mu}+1}$$

$$a_{11} = \frac{i\pi}{2}D_{11}, \qquad a_{10} = -\frac{i\pi}{2}D_{30}$$

$$W_4 = i\frac{a_{11}}{\pi}\bar{r}\sin\theta + D_{41}\frac{1}{\bar{r}}\sin\theta$$

$$D_{41} = \frac{i}{2}(D_{11})^2$$

$$a_{21} = \frac{i\pi}{2}D_{41}, \qquad a_{20} = -\frac{i\pi}{2}D_{70}, \qquad D_{70} = (D_{30})^2.$$

Also,

$$W_5 = -\frac{i}{6}\bar{y}^3 - \tfrac{1}{2}D_{11}r\ln\bar{r}\sin\theta + C_{51}\bar{r}\sin\theta + \frac{1}{\bar{r}}D_{51}\sin\theta + \frac{1}{\bar{r}^3}D_{53}\sin 3\theta$$

with

$$D_{51} = \frac{1}{\bar{\mu}+1}\left[C_{51}(\bar{\mu}-1) - \frac{i}{8}(3\bar{\mu}-1) - \tfrac{1}{2}\bar{\mu}D_{11} + \frac{1}{4}\frac{\bar{\mu}}{\bar{\rho}}D_{11}'\right]$$

$$C_{51} = \tfrac{1}{2}D_{11}\left(\frac{i\pi}{2} + \frac{1}{2} - \gamma + \ln 2\right)$$

$$D_{53} = \frac{i}{24}\frac{\bar{\mu}-1}{\bar{\mu}+1}$$

$$W_6 = D_{70}$$

$$W_7 = -\tfrac{1}{4}D_{30}\bar{r}^2 + D_{70}\ln\bar{r} + C_{70}$$

$$C_{70} = D_{70}(\gamma - \ln 2 - i\pi/2), \qquad D_{70} = (D_{30})^2.$$

The constants for the elliptical cavity are found by letting $\bar{\mu}\to\infty$ and $\bar{\rho}\to\infty$. This gives

$$D_{11} = ie^{\xi_0}\cosh\xi_0, \qquad D_{30} = \tfrac{1}{4}\sinh 2\xi_0$$

$$D_{32} = \tfrac{1}{8}e^{2\xi_0}\sinh 2\xi_0$$

$$D_{51} = e^{\xi_0}\left[-\frac{3i}{8}\sinh^2\xi_0\cosh\xi_0 + (C_{51} - D_{11}\xi_0/4)\cosh\xi_0 - \tfrac{1}{4}D_{11}\sinh\xi_0 + \tfrac{3}{32}D_{11}e^{-\xi_0}\right]$$

$$D_{53} = e^{3\xi_0}\left[\frac{i}{24}\sinh^2\xi_0\cosh\xi_0 + \tfrac{1}{96}D_{11}e^{-\xi_0}\right]$$

$$D_{72} = 0.$$

Абстракт — Рассматривается диффракция гармонических волн около эллиптического упругого цилиндра. Определяются, также, результаты для случая эллиптической полости. Даются численные результаты для напражений сдвига в цилиндре.